Lifetimes of electronically metastable double-Rydberg anions: FH_2^-

Maciej Gutowski[a] and Jack Simons[b]
Department of Chemistry, University of Utah, Salt Lake City, Utah 84112

(Received 8 March 1990; accepted 11 April 1990)

The method of analytic continuation of real stabilization graphs was applied to calculate positions and widths of electronic resonances of the FH_2^- double-Rydberg anion at the experimental geometry of the parent FH_2^+ cation. In correlated calculations on FH_2^-, a full configuration interaction calculation was performed on the two outermost electrons; the remaining electrons occupied orbitals taken from the SCF-level treatment of the FH_2^+ core. All spatial symmetries and both singlet and triplet spin multiplicities were considered. Many Feshbach and core-excited shape resonances were found with lifetimes in the range (1 to 80) $\times 10^{-14}$ s. Different methods of fitting the coefficients of the characteristic polynomial used in the stabilization calculations were considered. Techniques to suppress incomplete basis set artifacts in the stabilization calculations were examined.

I. INTRODUCTION

The FH_2^- anion is a potential member of the double-Rydberg (DR) anion family. Such species consist of an underlying closed-shell cation core around which a pair of highly correlated electrons move in diffuse orbitals. The first example of a molecular DR anion was observed in the Bowen group in 1987.[1,2] A low intensity, yet clearly identified, peak in the photoelectron spectrum of NH_4^- was interpreted as arising from a novel tetrahedral structure resembling the NH_4^+ cation with two diffuse electrons "orbiting" the cation core. Conjecture about the existence of a DR anion family[3] has been stimulated by experimental evidence from the Herzberg group who suggested the existence of stable Rydberg states of highly symmetric, neutral, polyatomic molecules.[4-6]

A few *ab initio* studies have been completed on the *ground states* of highly symmetric isomers of NH_4^- [3,7-11] and H_3O^- .[3,9,11,12] Both species were found to be locally geometrically stable (i.e., to be local minima on the respective potential energy hypersurfaces), to be electronically stable (i.e., to have lower electronic energy than the corresponding neutral Rydberg species at this geometry), but to be thermodynamically unstable and prone to fragmentation of the nuclear framework. For both species, the anion's extra electron is bound by ~ 0.5 eV, which is reasonable in view of the electron affinity of the isoelectronic sodium atom, 0.55 eV.[13]

Another step in the theoretical investigations of DR anions, undertaken in the present paper, aims at the *resonant* (electronically metastable) states. Here, we consider electronic resonances of the FH_2^- anion, which we have recently shown to be geometrically unstable in its ground state[11] [as is the neutral FH_2 in its $[^2A_1\,(4a_2)]$[14,11] ground state]. Both Feshbach resonances (i.e., metastable states lying below all neutral-molecule states to which decay can occur via one-electron ejection and hence, for which decay occurs via a two-electron process) and core-excited shape resonances (i.e., states which can decay via one-electron processes to a lower lying neutral-molecule state; in these cases, the ejected electron is temporarily bound by a centrifugal barrier) are examined.

In our resonance calculations, we use the method of analytic continuation of stabilization graphs[15] which is reviewed briefly in Sec. II. Extensive calculations for all spatial symmetries and for both singlet and triplet multiplicities were performed and are discussed in Sec. III. The results are summarized in Sec. IV.

II. METHODS

A. The stabilization technique

We use the analytic continuation of real stabilization graphs method to calculate resonance positions and lifetimes.[15-19] In this approach,[20] one finds eigenvalues of the molecular electronic Hamiltonian matrix within some specified energy range of interest. The calculations are repeated as the exponents of the Rydberg-like basis functions are varied by a uniform "scaling parameter" α. Stabilization graphs are plots of the roots $\{E_n\}$ of the secular equation

$$\det[\mathbf{H}(\alpha) - E\mathbf{S}(\alpha)] = 0 \tag{1}$$

as functions of the scaling parameter α. Both the Hamiltonian matrix $\mathbf{H}$ and the overlap matrix $\mathbf{S}$ depend on the scaling parameter because they depend on the basis set employed.

Given a stabilization graph in which two or more roots of the secular problem undergo avoided crossings, the real energies $\{E_n\}$ are analytically continued as functions of the scaling parameter and a search is undertaken for stationary points (i.e., complex values of α) at which

$$\left(\frac{dE_n}{d\alpha}\right)_{\alpha=\alpha_r} = 0. \tag{2}$$

These points are assumed to give, because coordinate-rotation theory[21] defines the meaning of the complex energies at such stable points, a metastable state's resonance position E_r and resonance lifetime τ,

[a] Permanent address: University of Warsaw, Department of Chemistry, Pasteura 1, 02-093 Warsaw, Poland.
[b] To whom correspondence should be addressed.

 0021-9606/90/162546-08$03.00

$$E_n(\alpha_s) = E_r - \frac{i\hbar}{2\tau}. \tag{3}$$

For typical one-open-channel resonances, for which an avoided crossing involves two curves only (one closed channel describing the resonance component and the open channel describing one state of an ejected electron and the neutral target molecule), the secular Eq. (1) may be simplified to the following quadratic form:

$$E^2 + P_1(\alpha)E + P_0(\alpha) = 0, \tag{4}$$

where

$$P_0(\alpha) = E_1(\alpha)E_2(\alpha), \tag{5}$$

$$P_1(\alpha) = -E_1(\alpha) - E_2(\alpha), \tag{6}$$

and E_1 and E_2 are the known roots of Eq. (1).[17]

It has been found in previous calculations[22,23] that polynomial approximations of P_1 and P_0 lead to satisfactory numerical results:

$$\overline{P}_1(\alpha) = \sum_{k=1}^{M} c_k \alpha^{k-1} \tag{7}$$

$$\overline{P}_0(\alpha) = \sum_{k=1}^{M} c'_k \alpha^{k-1}. \tag{8}$$

The coefficients c_k and c'_k can be determined either by choosing $2M$ roots from the stabilization graph and solving $2M$ simultaneous equations[22] or by a least-squares method[23] in which

$$\chi^2 = \sum_{i=1}^{N} [\overline{P}_k(\alpha_i) - P_k(\alpha_i)]^2, \quad k = 0,1 \tag{9}$$

is minimized. Here $2N$ is the number of the CI roots of the stabilization graphs, $\overline{P}_k(\alpha_i)$ is the polynomial approximation evaluated at α_i, and $P_k(\alpha_i)$ is either $E_1(\alpha_i)\,E_2(\alpha_i)$ or $-E_1(\alpha_i) - E_2(\alpha_i)$, where the $E_k(\alpha_i)$ are the actual CI energies at the real α_i values. An advantage of the later approach is that one can use many points from the stabilization graph without having to work with higher-order polynomials. In fact, it has been shown[16,22,23] that use of high order polynomials is generally not advantageous. In particular, determination of the resonance lifetimes is hindered when higher-order polynomials are employed.[18,22,23]

A potential drawback of employing χ^2 of Eq. (9) is that the resulting coefficients c_k and c'_k are not necessarily optimal for the functional

$$\chi^2 = \sum_{i=1}^{N} [\overline{E}_1(\alpha_i) - E_1(\alpha_i)]^2 + [\overline{E}_2(\alpha_i) - E_2(\alpha_i)]^2 \tag{10}$$

where the approximations to the CI roots E_1 and E_2 are given by

$$\overline{E}_{1,2} = \frac{-\overline{P}_1 \pm \sqrt{\overline{P}_1^2 - 4\overline{P}_0}}{2}. \tag{11}$$

The functional (10) is especially relevant because it focuses directly on the energy solutions to the secular matrix. Minimization of this functional is not a standard, nonlinear least-squares problem since Eq. (10) contains *two different* pieces, which depend on the same nonlinear parameters c_k and c'_k. The optimal parameters are determined in an iterative procedure using the optimal coefficients for the χ^2 of Eq. (9) as the first guess. The equations for this iterative procedure are given in the Appendix. The relative performance of the two alternatives to fitting are compared later in this paper.

After the real coefficients c_k and c'_k have been found, using real energies and real α values, we analytically continue the $\overline{P}_0$ and $\overline{P}_1$ polynomials into the complex plane. Then, using the stability equation, Eq. (2), with the solutions E_n approximated as in Eq. (11) but now the complex α values, the following equation for the optimal complex α_s is obtained:[11]

$$-\overline{P}_0\left(\frac{d\overline{P}_1}{d\alpha}\right)^2 + \overline{P}_1 \frac{d\overline{P}_0}{d\alpha}\frac{d\overline{P}_1}{d\alpha} - \left(\frac{d\overline{P}_0}{d\alpha}\right)^2 = 0. \tag{12}$$

Equation (12), which we solve using the Newton–Raphson method, has more than one solution. Substituting different solutions into Eq. (11) then, gives different resonance positions and lifetimes. Using low order fitting polynomials lessens the ambiguity in the resonance parameters resulting from the multiple solutions of Eq. (12) because the number of physically acceptable solutions rapidly decreases with polynomial order.

B. Electronic structure calculations

1. Atomic basis sets

All of our calculations were performed at the experimental geometry of the fluoronium ion FH_2^+ extracted from the gas phase infrared spectrum.[24] The HF distance is 0.967 Å and the HFH angle is 113.2°.

The atomic orbital basis set used resulted from combining the "core" Dunning $(12s6p/6s1p) \rightarrow [2s1p/3s1p]$ Gaussian basis set[25] with five sets of diffuse s,p, and d Gaussian functions centered on fluorine. Detailed information about the basis set is presented in Table I. The ability of these diffuse basis functions to reproduce Rydberg states was tested by using this basis to examine the H, Li, and Na atoms which have a large number of Rydberg excited states of well determined energy. It was found that the hydrogen energy levels for $n = 2,3$, and 4 were reproduced with errors less than 0.5%, 4.0%, and 11%, respectively. For Li and Na, we have reproduced, within 0.1 eV, the experimentally observed spacings of the lowest three ^2S and ^2P states and the lowest two ^2D states.

2. Basis scaling

To avoid unwanted changes of the underlying cation core orbitals and energy, scaling of the orbital exponents in the stabilization calculations was restricted to the more diffuse functions as identified in Table I. It is well established that incompleteness of the one- and many-electron basis set deteriorates the performance of the coordinate-rotation and stabilization methods.[26] In the case of the stabilization method, the resonance parts of the graphs are frequently not horizontal (i.e., α independent) because the energy of the target molecule is affected by the exponent scaling. Techniques for reducing such artifactual α dependence of the resonance energies are described later.

TABLE I. The Gaussian basis set used in the present calculations.

Center	Symmetry	Exponent	Contraction coefficients		Scaled?
F	*s*	745 30.0	9.500 00*E*-5	− 2.200 00*E*-5	No
		111 70.0	7.380 00*E*-4	− 1.720 00*E*-4	
		2543.00	3.858 00*E*-3	− 8.910 00*E*-4	
		721.000	1.5926*E*-2	− 3.748*E*-3	
		235.900	5.428 90*E*-2	− 1.2862*E*-2	
		85.6	1.495 13*E*-1	− 3.8061*E*-2	
		33.55	3.082 52*E*-1	− 8.6239*E*-2	
		13.93	3.948 53*E*-1	− 1.558 65*E*-1	
		5.915	2.110 31*E*-1	− 1.109 14*E*-1	
		1.843	1.715 10*E*-2	2.987 61*E*-1	
		0.7124	− 2.015*E*-3	5.850 13*E*-1	
		0.2637	8.690*E*-4	2.711 59*E*-1	
	p	80.390	6.3470*E*-3		No
		18.630	4.4204*E*-2		
		5.694	1.685 14*E*-1		
		1.953	3.615 63*E*-1		
		0.6702	4.421 78*E*-1		
		0.2166	2.434 35*E*-1		
	s,p,d	0.900*E*-0	1.0		Yes
	s,p,d	0.201*E*-0	1.0		Yes
	s,p,d	4.489*E*-2	1.0		Yes
	s,p,d	1.002*E*-2	1.0		Yes
	s,p,d	2.239*E*-3	1.0		Yes
H	*s*	82.64*E*-0	2.006 *E*-3		No
		12.41*E*-0	1.534 3*E*-2		
		2.824*E*-0	7.557 9*E*-2		
		7.977*E*-1	2.568 75*E*-1		
		2.581*E*-1	4.973 68*E*-1		
		8.989*E*-2	2.961 33*E*-1		
	s	2.581*E*-1	1.0		Yes
	s	8.989*E*-2	1.0		Yes
	p	1.0	1.0		No

3. Cation energy

In our calculations, all spatial symmetries and both singlet and triplet multiplicities of FH_2^- have been considered. To focus on the outer Rydberg pair of electrons, a self-consistent field (SCF) calculation was first performed on the fluoronium cation. This determined the reference energy of the cation species. Except as noted otherwise, all neutral and anion state energies are quoted relative to this cation energy in atomic units: 1 hartree = 27.21 eV.

4. Neutral FH_2 energies

Energies of the ground and excited states of neutral FH_2 were calculated at a level in which ten electrons occupy the cation's frozen $1a_1$, $2a_1$, $3a_1$, $1b_1$ and $1b_2$ SCF orbitals and one "active" electron is allowed to occupy an orbital whose energy is optimized. This, of course, results in a Koopman's theorem description of the 11th electron, a description that is consistent with the approximation used to describe the anion states (see below). We could, of course, have carried out more sophisticated calculations on the neutral states (in fact, we did to test the accuracy of the Koopmans-level energies). However, because our model for treating the many anion states of interest is based on treating only the outermost electron pair accurately, it was important to treat the neutral-molecule states in an analogous manner to be consistent.

5. Anion states

For the subsequent CI calculations on the anion, the orbitals that are occupied at the SCF level in the cation $1a_1$, $2a_1$, $3a_1$, $1b_1$, and $1b_2$ were frozen (i.e., their LCAO-MO coefficients were held constant) and ten electrons were used to occupy these orbitals in all configuration state functions. Next, full-CI calculations were performed for the two remaining electrons of the anion in the space of all other orbitals. The validity of this approach has been tested for the isoelectronic sodium anion and we have examined, for the FH_2^- ground state, the role of correlating other than the outermost electrons. The electron affinity of Na, measured in photoelectron spectroscopy experiments, is 0.548 eV,[13] whereas our calculation yields 0.547 eV. Calculations for metastable states of H^-, Li^-, and Na^- using the bases and tools described here served as further tests of the accuracy of our approach. For H^-, Li^-, and Na^-, discrepancies between experimental and our *ab initio* calculated resonance positions, measured relative to the neutral target levels, do not exceed a few hundredths of eV. Because FH_2^+ contains the same number of electrons and occupied orbitals as Na^+, it is unlikely that our treatment of the FH_2^+ core will lead to much larger errors than in Na^+, although the somewhat larger polarizability of FH_2^+ could give rise to errors that are two or three times those experienced for Na^+.

All of the *ab initio* calculations were performed using

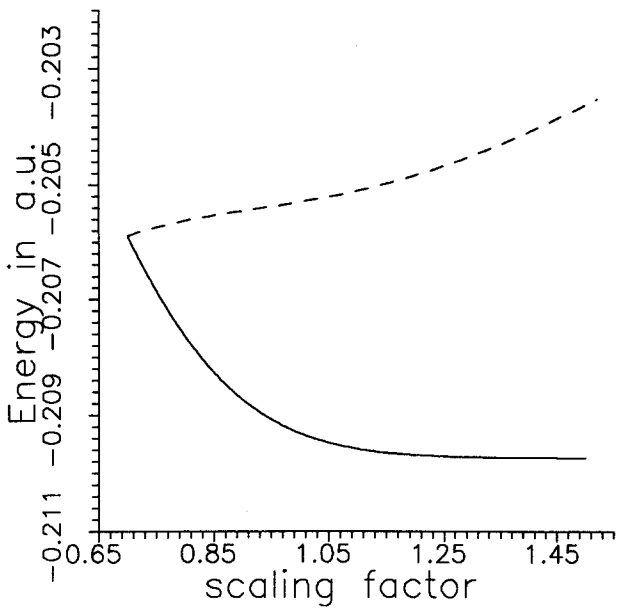

FIG. 1. Dependence of the $4a_1$ orbital energy (dashed line) on the scaling parameter α. Larger α values represent tighter orbitals. The SCF cation energies (solid line) have been shifted by a constant ($-$ 100.049 385 341 hartree) to match ϵ_{4a_1} at $\alpha = 0.70$ so the two graphs can appear in the same figure.

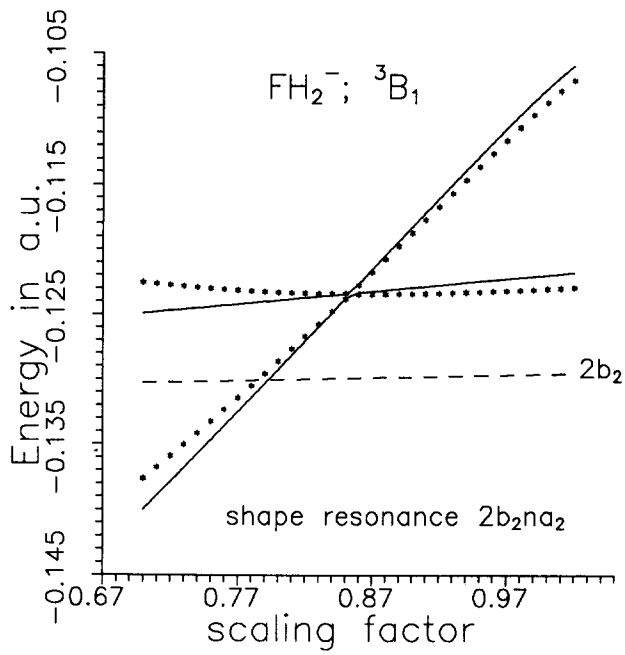

FIG. 3. Stabilization graphs for the CES $^3B_1$ ($2b_2na_2$) resonance obtained with and without the cation energy removed and labeled by the solid line and star symbols, respectively. The star symbols' positions have been obtained by shifting the computed anion energies by a constant ($-$ 100.257 644 375) hartree) equal to the cation energy at $\alpha = 0.85$.

our in-house Utah MESS KIT (molecular electronic structure kit) software modules[27] which we adapted to permit stabilization calculations and which we supplemented with an analytic continuation module.

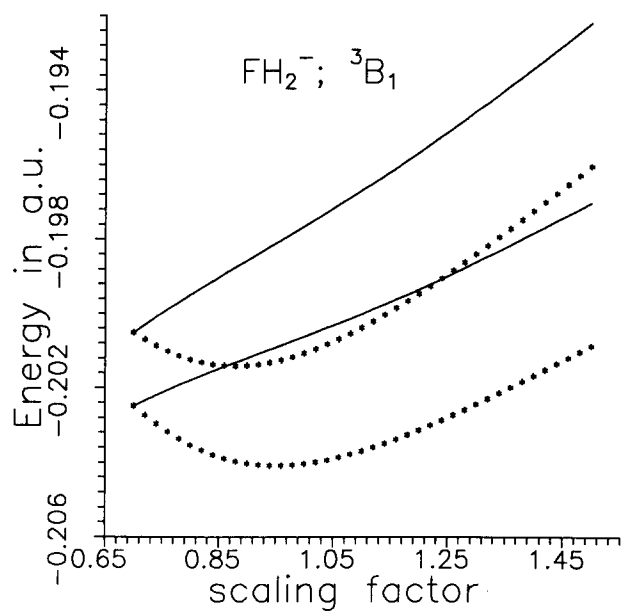

FIG. 2. The two lowest anion CI roots of $^3B_1$ symmetry (scattering states) with and without the cation energy removed and labeled by the solid line and star symbols, respectively. The star symbols' energies have been obtained by shifting the computed anion energies by a constant ($-$ 100.255 278 147 hartree) equal to the cation energy at $\alpha = 0.70$.

6. Removing artifactual α dependence

Initial stabilization calculations were performed for α values spaced by 0.05. Once the avoided crossings regions were located, we applied a finer grid (α values spaced by 0.01). Despite scaling the exponents of only the diffuse functions, the cation SCF energy still revealed a non-negligible dependence on α (see Fig. 1). Moreover, the energies of the neutral species, even if calculated with respect to the cation energy (i.e., with the artifactual α dependence of the cation removed), also displayed significant α dependence [e.g., the $^2A_1(4a_1)$ neutral state's energy is also presented in Fig. 1]. Therefore, it was necessary to introduce the following basis-set consistent technique to calculate resonance energies.

To overcome the unphysical α-dependence problems, we calculated all of the anion energies with respect to the α-dependent SCF cation energy since the bulk of the unphysical α dependence resides in the cation core's energy. In Fig. 2, the effectiveness of this technique is demonstrated for the two lowest, nonresonant anion roots of $^3B_1$ symmetry. A comparison of the stabilization graphs for a core-excited shape (CES) resonance of $^3B_1$ symmetry (having a dominant $2b_2na_2$ configuration) obtained with and without the cation energy removed is given in Fig. 3. It should be mentioned that when specifying electron configurations using notation such as $2b_2na_2$, we attempt to indicate that one of the Rydberg-type electrons is usually on the $2b_2$ orbital whereas the second is distributed among the a_2 orbitals having energy higher than ϵ_{2b_2}.

One might wonder why the neutral's energy is not subtracted from the anion energy to achieve a more α-indepen-

TABLE II. Energies E_r (hartrees) and lifetimes τ (10^{-14} s) for the $^1A_1(6a_1^2)$ Feshbach resonance calculated with the Mth order fitting polynomials $\bar{P}_0$ and $\bar{P}_1$ obtained using Eqs. (9) and (10). The α range was 1.03–1.09 and the points were spaced 0.01 apart. The abbreviation p.u.s. stands for "physically unacceptable solution."

M	Eq. (9)		Eq. (10)	
	E_r	τ	E_r	τ
2	p.u.s.		−0.079 18	35
3	−0.079 17	35	−0.079 17	34
4	−0.079 15	19	−0.079 17	32
5	p.u.s.		−0.079 17	33

dent stabilization graph. Such an approach is certainly appropriate if *only one* electronic state of the neutral target is involved in resonant scattering. For example, the resonance state depicted in Fig. 3 has a dominant component connected to the neutral $^2B_2$ ($2b_2$) state. In contrast, the $^3B_1$ CES resonant wave function with energy −0.9025 hartree (see Table III) is dominated by $2b_1na_1$ and $5a_1nb_1$ electron configurations. In this case, it is difficult to decide whether the $^2B_1$ ($2b_1$) or $^2A_1$ ($5a_1$) energy of the target should be subtracted from the anion energy. It is because of such potential ambiguity and because the cation core energy contains most of the unphysical α dependence that we choose to reference all energies to the α-scaled cation energy.

The performance of the analytic continuation method with the $\bar{P}_0$ and $\bar{P}_1$ polynomials optimized for the two weight functions defined in Eqs. (9) and (10) is compared in Table II for the $^1A_1$ ($6a_1^2$) Feshbach resonance (see the stabilization graph in Fig. 4). It is observed that the resonance positions and lifetimes obtained in the later approach are much less dependent on the order M of the fitting polynomials. Moreover, for some M's the approach based on Eq. (9) does not yield any physically acceptable resonance parameters.[28] For this reason, all of the results discussed from here on were obtained using the fitting procedure characterized by Eq. (10).

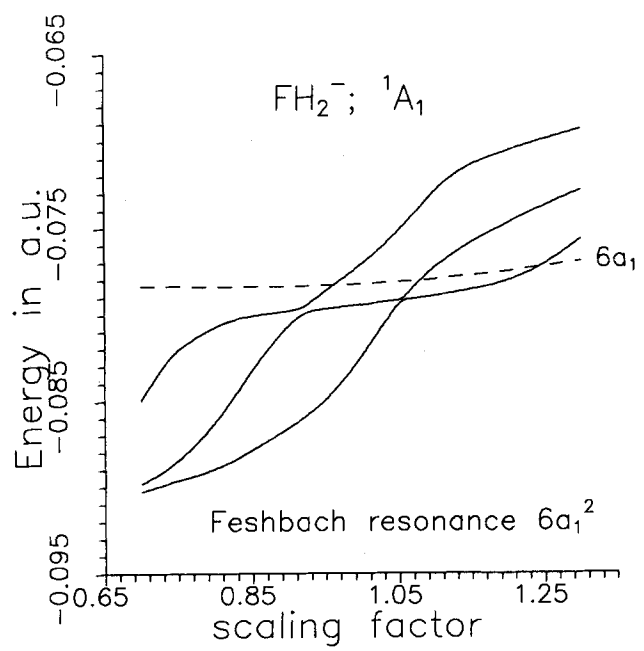

FIG. 4. Stabilization plot for the longest lived Feshbach $^1A_1$ ($6a_1^2$) resonance. The energy of the nearby neutral state is depicted by a dashed line.

III. RESULTS

In Table III we characterize the low lying singlet and triplet resonances that we found for FH_2^- states of A_1, A_2, B_1, and B_2 symmetries, and in Figs. 4–8 we present selected pertinent stabilization graphs. The resonance positions are given (in hartree units) relative to the parent cation's energy, and the dominant electronic configurations are shown to specify the electronic states of the FH_2 target that could be involved in resonant electron scattering.

Analogous calculations for metastable states of H^-, Li^-, and Na^- served as a measure of the accuracy of the above approach. For these systems, discrepancies between experimental and our *ab initio* calculated resonance positions, measured relative to the neutral target levels, do not exceed a few hundredths of eV. Also, our resonance lifetimes are quantitatively correct for these atomic anions. For instance, for the most frequently studied ^1S ($2s^2$) metastable state of H^- our resonance parameters are −0.629 eV and 12×10^{-14} s for resonance position and lifetime, respectively, whereas the benchmark results are −0.647 eV and 14×10^{14} s.[22]

We have found several singlet and triplet Feshbach and CES resonances which decay to geometrically stable excited states of the neutral target. No shape resonances (i.e., resonances of the shape variety with the ground state of the neutral as the parent) emerged from our calculations.

The longest lived Feshbach resonance is of $^1A_1$ ($6a_1^2$) symmetry (Fig. 4) and its lifetime is 34×10^{14} s. Among the five Feshbach resonances that we found, three have been classified as two-open-channel species, (see Figs. 5 and 6 and Table III). The $^3A_1$ ($5a_1na_1$) resonance (Fig. 5) can decay via ejection of an electron either to the ground $^2A_1$ ($4a_1$) state of the neutral, or to the first excited $^2B_2$ ($2b_2$) state. The former and the latter channels are reflected in Fig. 5 in the steeply and less steeply rising branches of the stabilization graph, respectively. The slopes of these branches reflect the different kinetic energies of the ejected electron. In Fig. 6, two other two-open-channel resonances of $^3B_1$ ($2b_1na_1$) symmetry are displayed. For such two-open-channel cases, the total decay rate depends on the coupling of the resonant wave function with *both* open channels. Hence, the one-open-channel method formulated in Sec. II, when used to estimate the decay rate to each open channel independently, allows for only a qualitative estimate of the resonance parameters. Such results are presented in Table III.

The CES resonances reported in Table III frequently appear in clusters of two or three states (see Figs. 7 and 8). These clusters correspond to states of the same spatial and spin symmetry and are different solutions of the Schrödinger equation for the same neutral target states and with the same centrifugal barrier. For such resonances lying above the neutral $^2B_1$ ($2b_1$) state, the resonant wave function frequently

TABLE III. Metastable state symmetries, types,[d] energies, and lifetimes for double Rydberg H_2F^-.

Symmetry	Type	Configuration[a]	Energy[b]	Lifetime[c]
$^1A_1$	CES	$2b_2nb_2$	−0.123 69	3
$^1A_1$	CES	$2b_2nb_2$	−0.119 33	7
$^1A_1$	F	$6a_1^2$	−0.079 17	34
$^3A_1$	CES	$2b_2nb_2$	−0.125 13	14
$^3A_1$	CES	$2b_2nb_2$	−0.123 26	32
$^3A_1$	F	$5a_1na_1$		
	($4a_1ka_1$ channel)		−0.098 86	1
	($2b_2kb_2$ channel)		−0.098 81	5
$^1A_2$	CES	$2b_1nb_2$	−0.094 71	14
$^1A_2$	CES	$2b_1nb_2$	−0.091 57	80
$^1A_2$	CES	$5a_1na_2$	−0.089 46	26
$^3A_2$	CES	$2b_1nb_2$	−0.094 26	18
$^3A_2$	CES	$2b_1nb_2$	−0.091 59	19
$^3A_2$	CES	$5a_1na_2$	−0.089 59	24
$^1B_1$	F	$2b_1na_1$	−0.100 69	4
$^3B_1$	CES	$2b_2na_2$	−0.123 39	17
$^3B_1$	F	$2b_1na_1$		
	($2b_2ka_2$ channel)		−0.101 45	8
	($4a_1kb_1$ channel)		−0.102 55	1
$^3B_1$	F	$2b_1na_1$		
	($2b_2ka_2$ channel)		−0.097 82	10
	($4a_1kb_1$ channel)		−0.097 96	6
$^3B_1$	CES	$2b_1na_1 + 5a_1nb_1$	−0.090 25	17
$^3B_2$	CES	$2b_2na_1$	−0.125 80	11
$^3B_2$	CES	$2b_2na_1$	−0.122 97	2
$^3B_2$	CES	$2b_1na_2 + 5a_1nb_2$	−0.092 41	14
$^3B_2$	CES	$2b_1na_2 + 5a_1nb_2$	−0.090 92	46
$^3B_2$	CES	$2b_1na_2 + 5a_1nb_2$	−0.089 10	7

[a] The notation $n\lambda$ ($\lambda = a_1, a_2, b_1$ or b_2) is used to indicate that one Rydberg-type electron is distributed among many λ-symmetry orbitals.
[b] The energies are given relative to the parent cation species (in hartrees) in all cases.
[c] The lifetimes are given in units of 10^{-14} s. A lifetime of 10^{-14} s corresponds to an energy width of 0.066 eV in the resonance.
[d] Feshbach (F) and core-excited shape (CES).

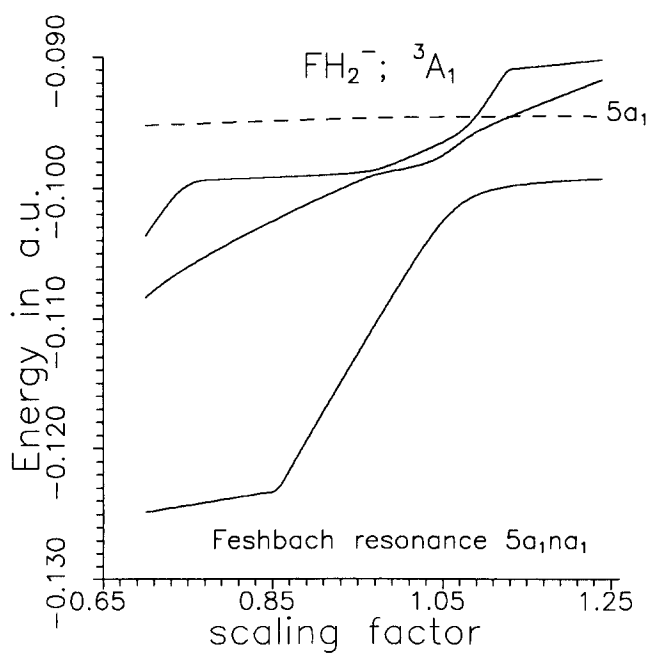

FIG. 5. Stabilization graph for the two-open-channel Feshbach $^3A_1$ ($5a_1na_1$) resonance. The energy of the nearby neutral state is depicted by a dashed line.

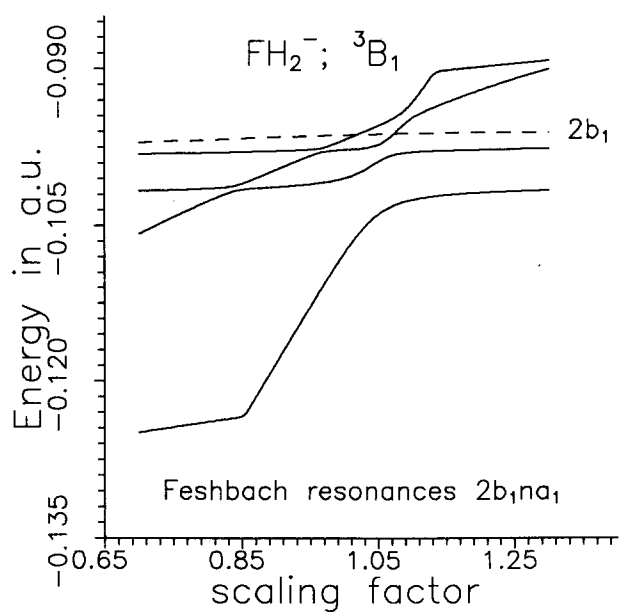

FIG. 6. Stabilization graphs for two two-open-channel Feshbach $^3B_1$ ($2b_1na_1$) resonances. The energy of the nearby neutral state is depicted by a dashed line.

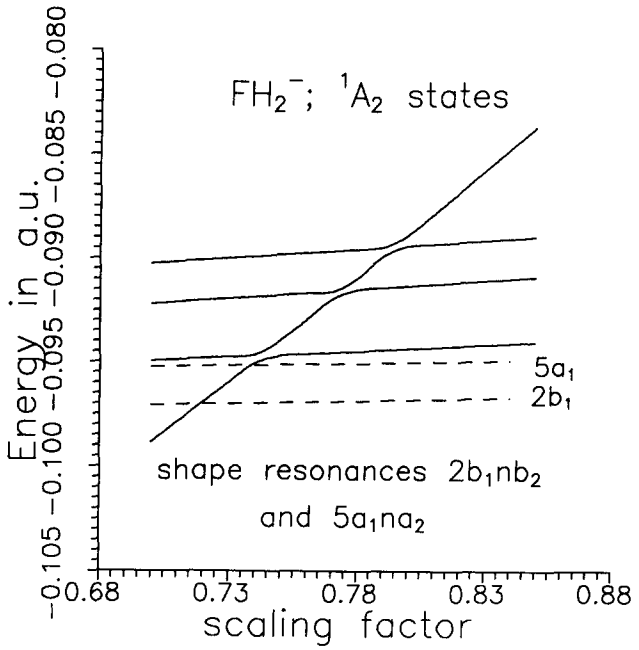

FIG. 7. Three-term cluster of CES $^1A_2$ resonances. The two lower resonances are dominated by $2b_1nb_2$ electron configurations. The highest one has $5a_1na_2$ character. The middle one is the longest lived CES resonance. The energies of nearby neutral states $2b_1$ and $5a_1$ are depicted by dashed lines.

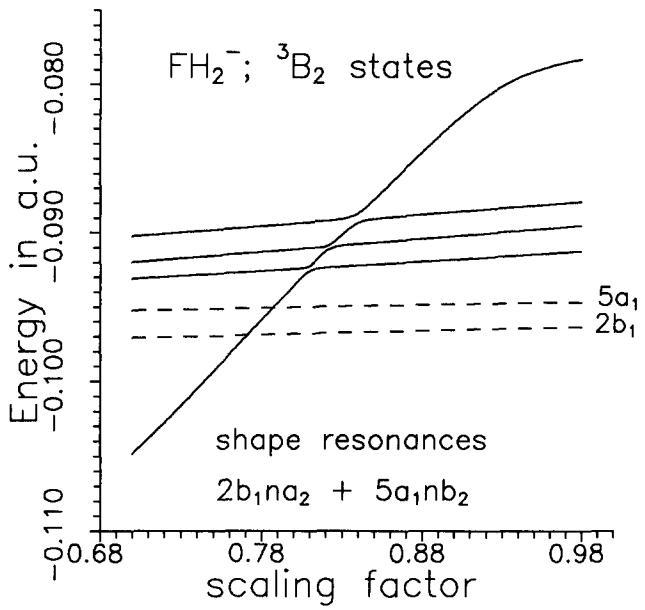

FIG. 8. Three-term cluster of CES $^3B_2$ $2b_1na_2 + 5a_1nb_2$ resonances. The energies of nearby neutral states $2b_1$ and $5a_1$ are depicted by dashed lines.

displays "multiconfiguration" character because the next neutral level, $[^2A_1\ (5a_1)]$, is only 0.04 eV higher in energy, and therefore, contributes heavily to the resonant wave function (see Fig. 8). The longest lived CES resonance is the $^1A_2$ $(2b_1nb_2)$ state (Fig. 7) with a lifetime of 80×10^{-14} s.

On the basis of the range of lifetimes found here, it is expected that electronically metastable states of FH_2^- can display vibrational and may even show some rotational structure. Since the ground states of the FH_2^- anion and FH_2 neutral are geometrically unstable near the cation equilibrium geometry, the observation of the CES and Feshbach resonances studied here could probably not be realized using standard photoelectron or photodetachment techniques. However, experiments in which ground-state FH_2^+ is used to produce, via double charge exchange, metastable states of FH_2^- may be a fruitful avenue of approach. Alternatively, an approach using electron attachment to excited Rydberg states of neutral FH_2, which were predicted to be geometrically stable,[11,14] may be successful.

IV. CONCLUSIONS

We used the method of analytic continuation of stabilization graphs to investigate electronic resonances in the double-Rydberg structure of FH_2^-. Many Feshbach and core-excited shape resonances have been found with lifetimes in the range (1 to 80) $\times10^{14}$ s. Among the Feshbach-type species a few two-open-channel resonances have been observed. Proper treatment of the latter resonances requires further formal development of the analytic continuation method.

Selected numerical aspects of the method as applied to one-open-channel cases have been carefully studied. A new approach aimed at suppressing incomplete basis-set artifacts has been proposed. Different ways of fitting the coefficients of the characteristic polynomials used in the analytic continuation process have been tried, and the subsequent stability of the resonance parameters have been examined.

From the experimental perspective, studies of these anionic metastable states present significant challenges. Our results suggest that double charge exchange methods or experimental control over excited states of neutral FH_2 may be necessary before studies of these anionic resonances will be possible. It is our desire to nurture interest in these systems within the experimental community.

ACKNOWLEDGMENTS

The authors acknowledge the financial support of the National Science Foundation (Grant No. CHE8704779) and the office of Naval Research. M. G. has been also supported by the Polish Academy of Sciences with Grant No. CPBP 01.12.

APPENDIX

Optimization of the nonlinear parameters c_k and c_k' for the weight function of Eq. (10) is performed in an iterative manner starting from the coefficients optimized for the weight function of Eq. (9). The current coefficients are collected into vector $\mathbf{c}^{cur}$ and equations for the corrections Δc_k's are obtained through minimization of the χ^2 function of Eq. (10) with respect to the Δc_k's, with $\overline{E}_1$ and $\overline{E}_2$ replaced by their Taylor expansions around $\mathbf{c}^{cur}$ truncated after the linear terms. The resulting equations have the form

$$\sum_{k=1}^{2M} G_{lk}\Delta c_k = B_l, \quad l = 1,...,2M, \tag{A1}$$

where

$$\mathbf{G} = \mathbf{G}_1 + \mathbf{G}_2 \tag{A2}$$

and

$$\mathbf{B} = \mathbf{B}_1 + \mathbf{B}_2. \tag{A3}$$

Using the index m to label the two branches 1 or 2 of the avoided crossing, the $\mathbf{G}_m$ and $\mathbf{B}_m$ elements are given by

$$\mathbf{G}_m = \mathbf{A}_m^T \mathbf{A}_m \tag{A4}$$

$$\mathbf{B}_m = \mathbf{A}_m^T \mathbf{b}_m. \tag{A5}$$

The (ith and k th) element of the $\mathbf{A}_m$ matrix is given by

$$A_{m,ik} = \left(\frac{\partial \overline{E}_m}{\partial c_k} \right)_{\alpha_i, \mathbf{c}^{\mathrm{cur}}} \tag{A6}$$

and the ith element of vector $\mathbf{b}_m$ is defined as

$$b_{m,i} = E_m(\alpha_i) - \overline{E}_m(\alpha_i, \mathbf{c}^{\mathrm{cur}}). \tag{A7}$$

The next iterations's approximation to the fitting parameters are then given by

$$c_k^{\mathrm{next}} = c_k^{\mathrm{cur}} + \Delta c_k, \quad k = 1,...,2M. \tag{A8}$$

The procedure given by Eqs. (A1)–(A8) is repeated until the χ^2 of Eq. (10) reaches a minimum as indicated when the norm of $\Delta\mathbf{c}$ becomes smaller than some threshold at a point where the $\mathbf{G}$ matrix is positive definite.

[1] S. T. Arnold, J. G. Eaton, D. Patel-Misra, H. W. Sarkas, and K. H. Bowen, in *Ion and Cluster Ion Spectroscopy and Structure*, edited by J. P. Maier (Elsevier, New York, 1989).

[2] K. H. Bowen and J. G. Eaton, in Proceedings of the International Workshop on the Structure of Small Molecules and Ions, Jerusalem, Israel, 1987.

[3] M. Gutowski, J. Simons, R. Hernandez, and H. L. Taylor, J. Phys. Chem. **92**, 6179 (1988).

[4] G. Herzberg, J. Chem. Phys. **70**, 5806 (1979).

[5] G. Herzberg, Faraday Discuss. Chem. Soc. **71**, 165 (1981).

[6] G. Herzberg, Ann. Rev. Phys. Chem. **38**, 27 (1987).

[7] J. Kalcher, P. Rosmus, and M. Quack, Can. J. Phys. **62**, 1323 (1984).

[8] H. Cardy, C. Larrieu, and A. Dargelos, Chem. Phys. Lett. **131**, 507 (1986).

[9] D. Cremer and E. Kraka, J. Phys. Chem. **90**, 33 (1986).

[10] J. V. Oritz, J. Chem. Phys. **87**, 3557 (1987).

[11] M. Gutowski and J. Simons, J. Chem. Phys. (in press).

[12] J. V. Oritz, J. Chem. Phys. **91**, 7024 (1989).

[13] T. A. Patterson, H. Hotop, A. Kasdan, D. W. Norcross, and W. C. Lineberger, Phys. Rev. Lett. **32**, 189 (1974).

[14] I. D. Petsalakis, G. Theodorakopoulos, J. S. Wright, and I. P. Hamilton, J. Chem. Phys. **89**, 6841 (1988); **88**, 7633 (1988).

[15] J. Simons, J. Chem. Phys. **75**, 2465 (1981).

[16] R. F. Frey and J. Simons, J. Chem. Phys. **84**, 4462 (1986).

[17] C. W. McCurdy and J. F. McNutt, Chem. Phys. Lett. **94**, 306 (1983).

[18] A. D. Isaacson and D. G. Truhlar, Chem. Phys. Lett. **110**, 130 (1984).

[19] P. O. Lowdin, Int. J. Quant. Chem. **27**, 495 (1985).

[20] H. S. Taylor, Adv. Chem. Phys. **18**, 91 (1970).

[21] W. P. Reinhardt, Ann. Rev. Phys. Chem. **33**, 223 (1982).

[22] J. Bentley and D. M. Chipman, J. Chem. Phys. **86**, 3819 (1987).

[23] P. Froelich, K. Szalewicz, B. Jeziorski, W. Kolos, and H. J. Monkhorst, J. Phys. B **20**, 6173 (1987).

[24] E. Schafer and R. J. Saykally, J. Chem. Phys. **81**, 4189 (1984).

[25] T. H. Dunning (unpublished results).

[26] D. T. Chuljian, and J. Simons, Int. J. Quant. Chem. **23**, 1723 (1983).

[27] UTAHMOD: The Utah Mess KIT software was written during 1986–1988 primarily by R. A. Kendall, E. Earl, R. Hernandez, H. L. Taylor, D. O'Neal, Dr. J. Nichols, and Dr. M. Hoffmann.

[28] An initial estimate of the resonance parameters may be obtained from Simons' graphical approach (see Ref. 15).